THE CREEP–FATIGUE BEHAVIOR OF COMMERCIAL AND P–DOPED 304L STAINLESS STEEL

J. J. Kim* and S. W. Nam*

The creep–fatigue interaction of commercial and P–doped 304L stainless steel was studied at the test temperature of 823 K. The results of continuous fatigue tests showed that the effect of P on the fatigue life was proven to be detrimental. But the results of creep–fatigue test for the two materials show that the effect of P is beneficial for the fatigue life under creep–fatigue interaction condition. Since the segregation of P on grain boundary lowers grain boundary diffusivity and the density of grain boundary precipitates, the nucleation and growth rate of cavity of P–doped 304L stainless steel is considered to be slower than that of commercial 304L stainless steel. Therefore, the addition of P to 304L stainless steel is believed to prolong the creep–fatigue life.

INTRODUCTION

For 304 stainless steel under creep–fatigue loading conditions, it has been generally accepted that cavity nucleation and growth during hold time degrades the fatigue endurance and the formation of cavities is closely related to the intergranular carbide precipitates. Because the carbon content of 304L stainless steel is about half of that of 304 stainless steel, there is considerably low density and small size of grain boundary carbide precipitates. Therefore, it is expected that the creep–fatigue behaviors of the two materials may be different, and this difference would explain the role of carbide precipitates for the creep–fatigue interaction.

In the structural alloys in nuclear reactor, sometimes, the segregation of P at the surface and grain boundary induced by the irradiation was observed [1,2]. In a recent study on the creep behavior of 304 stainless steel [3], the segregation of P at the grain boundaries accelerates the cavity nucleation rate. However, there appears to be less information published in the literature for the effects of impurities such as P on the creep–

* Department of Materials Scinnce & Engineering,
Korea Advanced Institute of Science & Technology, Seoul, Korea

fatigue interaction behavior.

The work reported here examines the creep–fatigue behavior of commercial and P–doped 304L stainless steel at 823 K. The purpose of this paper is to investigate the effects of P on the carbide formation characteristics and in turn on the creep–fatigue behavior of 304L stainless steel.

EXPERIMENTAL

Two experimental heats based on a commercial grade type 304L stainless steel were produced in an induction furnace with compositions shown in Table I.

Table I. Chemical composition of commercial and P-doped type 304L stainless steel (wt%)

Material	C	Si	Mn	P	S	Cr	Mo	Ni
commercial	0.026	0.32	1.16	0.028	0.018	18.09	0.42	9.3
P-doped	0.029	0.30	1.10	0.209	0.020	18.00	0.39	9.2

The procedure of specimen preparation are given in detail elsewhere [4]. The specimen is fabricated to be cylindrical with a gauge length of 8 mm. The average grain size of the two materials was measured to be 120μm. The specimens were aged at 1033 K for 50 h to allow the formation of a well defined grain boundary carbide that was stable during the subsequent experiments. For brevity, the commercial 304L stainless steel and the P–doped 304L stainless steel will hereafter be called CSS and PSS, respectively. The typical microstructures of heat treated CSS and PSS are shown in Fig.1. In PSS, some large planar carbides are observed at grain boundary triple points. But the density of equiaxed carbide precipitated at grain boundary is higher in CSS.

All the fatigue tests were conducted on an electromechanically driven closed loop INSTRON Model 1362 under an applied total strain amplitude control mode. Strain was monitored with an extensometer, the strain wave form was a symmetrical triangular shape of tension and compression and the strain rate was fixed to be $4 \times 10^{-3}/s$. For the investigation of the phenomenon of creep–fatigue interaction, 30 min hold at tensile peak strain was applied. To prevent oxidation, all the tests were carried out in high purity argon atmosphere (matheson 99.999%).

The characteristic morphology of the fracture surface and the cavitation behavior during creep–fatigue cycling were examined by scanning electron micrography.

A PHI model 590 scanning Auger microprobe (SAM) was used for analysis of phosphorus segregated at the grain boundary.

RESULTS AND DISCUSSION

In order to investigate the effect of P addition on the cavitation behavior of 304L stainless steel, we detected the segregation of P and all other elements. The results of the chemical analysis at the grain boundary of the two materials by Auger electron spectroscopy are shown in Table II. Auger peak height ratios and at% for all elements are summarized.

Table II. Atomic fraction of elements at grain boundary

		CSS		PSS	
	scale factor	peak height ratio	atomic fraction	peak height ratio	atomic fraction
P	0.47	0.027	0.0083	0.066	0.0203
S	0.75	0.073	0.0139	0.049	0.0095
C	0.14	0.036	0.0371	0.033	0.0371
Cr	0.31	0.409	0.1949	0.426	0.2000
Ni	0.27	0.182	0.0962	0.139	0.0751
Fe	0.22	1.000	0.6496	1.000	0.0751

It is shown that only the concentration of P is dominantly increased in PSS and the others are similar in the two materials.

Impurity segregation at the grain boundary and surface directly influence the cavity nucleation and growth kinetics through their effects on the interfacial energy and diffusivity. From the results of Auger spectroscopy tests for the two materials (Table II), it is shown that the addition of P to 304L stainless steel does not significantly change the grain boundary concentration of the other elements. Therefore, it can be assumed that all elements except P act like pure solvent, that is, for simplicity, the segregation of P at grain boundary of 304L stainless steel can be treated using the thermodynamics for dilute binary solid solutions.

From the combination of Gupta's suggestion [5] and McLean isotherm [6] for dilute binary solid solution and the result of Auger spectroscopy test, we can get

$$\gamma_b^{CSS} - \gamma_b^{PSS} = 0.020$$

where γ_b is grain boundary energy. And the ratio of the effective grain bounday diffusivity of the two materials is obtained as

$$\frac{\delta D_b^{CSS}}{\delta D_b^{PSS}} = 1.60$$

where δ is the effective width of grain boundary. These effects are to be discussed in connection with the cavity nucleation and growth mechanisms.

Fig.2 shows the continuous low cycle fatigue and creep–fatigue lives of the two materials at the various total strain ranges. The life of CSS under creep–fatigue cycling is significantly reduced compared with the life under continuous cycling, and it is observed that the ratio of the reduction of the lives is higher with lower strain amplitude. The life of PSS in creep–fatigue condition is also reduced in similar manner compared to that in continuous cycling condition, but the ratio of the reduction is much smaller than that of CSS. Not only this but there is another very interesting result observed for PSS, that is, the life of PSS under creep–fatigue condition is observed to be longer than that of CSS, though the addition of P in commercial alloys generally reduced the fracture toughness by grain boundary segregation.

Generally, the intergranular crack growth under creep–fatigue cycling is related to the cavities which are nucleated and grown during tensile hold time [7,8]. Accordingly, the size and distribution of cavities can be a measure to assess the creep–fatigue interaction.

Fig.3 shows the fractured surface by impact and the crack surfaces of the two materials tested at $\Delta\varepsilon_t$ of $\pm 2.0\%$ with t_h of 30 min. Cavities grown comparatively large are viewed at grain boundaries of CSS fractured by impact (Fig.3(a)). Fig.3(c) and Fig.3(d) show the crack surfaces of CSS and PSS, respectively. Arrows indicate direction of crack advance. It is observed that the cavities are linked along the direction of crack advance in both materials.

In order to interpret the creep–fatigue behavior of the two materials, we consider the quantitative equations for the cavity nucleation kinetics and the growth rate.

In our creep–fatigue tests, we use the strain rate $\dot{\varepsilon}$ of $4 \times 10^{-3}/s$ at all conditions and this value is much higher than the critical strain rate, $\dot{\epsilon}_c$ for fatigue cavity nucleation [9]. Accordingly, it seems that the nucleation of cavity during continuous cycling does not occur. Therefore, we apply the general theory of nucleation kinetics [10] to cavity nucleation during hold time, and we get $J_\circ^{PSS}/J_\circ^{CSS} = 0.9$ at $\Delta\varepsilon_t$ of $\pm 2.0\%$ where $J_\circ$ represents the steady state nucleation rate. This lower nucleation rate of P–doped 304L stainless steel is mainly due to the decrease of the number of grain boundary precipitates by the addition of P.

On the other hand, from the results of creep–fatigue tests for CSS and PSS, we could observe that the stress relaxation is very small during hold time. Therefore, the effect of the plastic deformation on cavity growth behavior can be neglected and the growth of cavity is considered to be controlled by grain boundary diffusion. From Hull and Rimmer

equation [11] which is good approximation for grain boundary diffusion controlled growth rate of cavity, if we consider the case of the same cavity size and same inter–spacing, we can get $(dV/dt)^{PSS}/(dV/dt)^{CSS} = 0.7$.

From the above stated considerations for cavity nucleation and growth kinetics of CSS and PSS, it can be found that since the addition of P to 304L stainless steel lowers the nucleation and growth rate of cavity, the creep–fatigue life of PSS is longer than that of CSS at the same total strain range. This coincides well with Fig.2 which shows the results of creep–fatigue tests.

SYMBOLS USED

$\Delta\varepsilon_t$ = total strain range
γ_b = grain boundary energy
δD_b = effective grain boundary diffusivity
J_o = steady state nucleation rate
V = volume of cavity

REFERENCES

1) J. L. Brimhall, D. R. Baer and R. H. Jones, J. Nucl. Mater., v.117, 1983, p.218
2) J. L. Brimhall, D. R. Baer and R. H. Jones, J. Nucl. Mater., v.122& 123, 1984, p.196
3) J. H. Hong, S. W. Nam, and S. P. Choi, J. Mater. Sci., v.21, 1986, p.3966
4) J. J. Kim and S. W. Nam, Scripta Metall., v.23, 1989, p.1437
5) D. Gupta, Metall. Trans., v.8A, 1977, p.1431
6) D. McLean, in 'Grain Boundaries in Metals', Oxford University Press, London, 1957
7) B. K. Min and R. Raj, Acta Metall., v.26, 1978, p.1007
8) J. Wareing, Met. Trans., v.8A, 1977, p.711
9) N. Y. Tang, D. M. R. Taplin and A. Plumtree, Mater. Sci. Technol., vol. 1, 1985, p.145
10) J. W. Christian, in 'The Theorey of Transformations in Metals and Alloys', 2nd edn., Part 1, Pergamon Press, Oxford, 1975, p.418
11) D. Hull and D. E. Rimmer, Phil. Mag., v.4, 1959, p.673

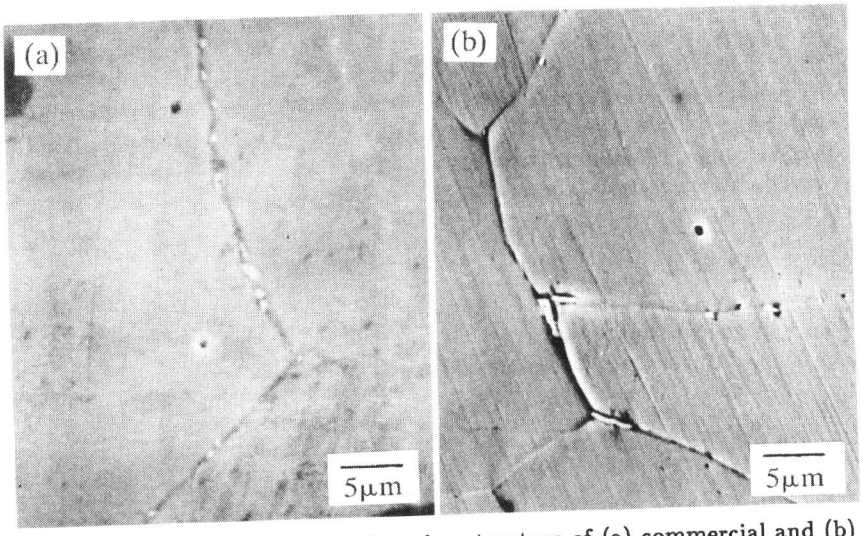

Fig. 1. SEM micrographs for the microstructure of (a) commercial and (b) P–doped 304L stainless steel.

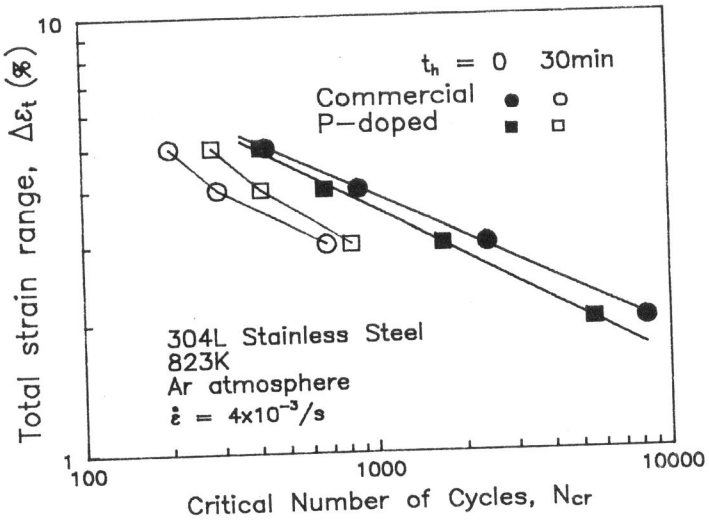

Fig. 2. Creep–fatigue life of commercial and P–doped 304L stainless steel at various total strain range.

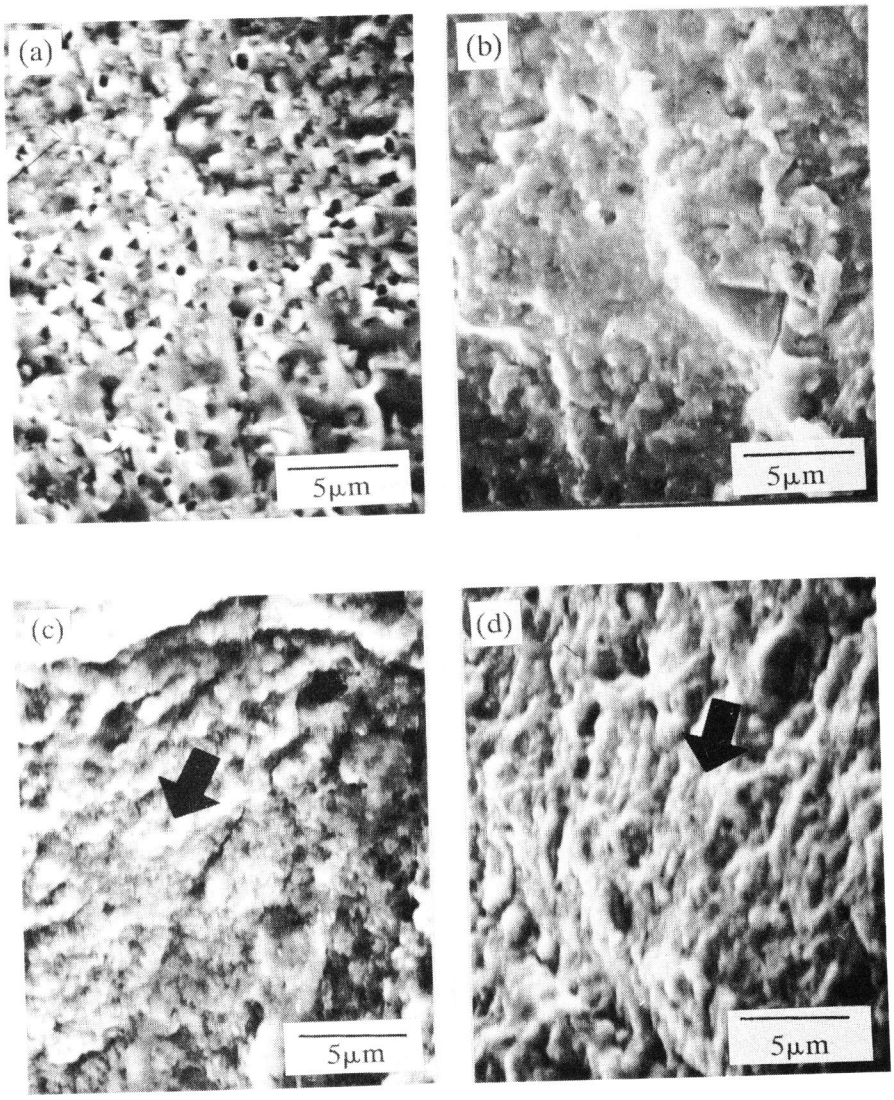

Fig. 3. SEM micrographs for the fatigue fractured surface and the surface separated by impact at LNT after creep–fatigue testing.
(a) impact fractured, commercial (b) impact freactured, P–doped
(c) C–F fractured, commercial (d) C–F fractured, P–doped